Available online at www.sciencedirect.com

SCIENCE DIRECT®

International Journal of Mass Spectrometry 244 (2005) 41–49

www.elsevier.com/locate/ijms

Secondary ion emission from CO_2–H_2O ice irradiated by energetic heavy ions
Part II: Analysis–search for organic ions

C.R. Ponciano, L.S. Farenzena, V.M. Collado, E.F. da Silveira*, K. Wien[1]

Physics Department, Pontifícia Universidade Católica, 22543-970 Rio de Janeiro, Brazil

Received 22 January 2005; accepted 7 April 2005
Available online 17 May 2005

Abstract

Secondary ion mass spectrometry is used to investigate ion emission from a frozen-gas mixture of CO_2 and H_2O ($T = 80$–90 K) bombarded by MeV nitrogen ions and by ^{252}Cf fission fragments. The aim of the experiment is to detect organic molecules, produced in the highly excited material around the nuclear track, which appear as ions in the flux of sputtered particles. Part I of the present work [L.S. Farenzena, V.M. Collado, C.R Ponciano, E.F. da Silveira, K. Wien. Int. J. Mass Spectrom. 243 (2005) 85–93] described the method and presented the time-of-flight mass spectra; a list of the CO_2 specific and H_2O specific reaction products was provided. In Part II, the peaks of the TOF mass spectra are analyzed.

Projectile-ice direct coulomb interaction leads to the production in the track of the H^+, C^+, O^+, O_2^+, CO^+ and CO_2^+ primarily ions, which react in the highly energized nuclear track plasma mainly with CO_2 and H_2O or H_2CO_3. The positive molecular hybrid ions formed are identified as organic species like COH^+, $COOH^+$, $CH_{n=1\text{–}3}^+$, $H_{n=1,2}COOH^+$ and cluster ions. Similarly, the negative primarily ions O^- and OH^- formed by electron capture produce negative hybrid ions such as $(CO_2)_nOH^-$, the four ions $(CO_4H_{m=0\text{–}3})^-$ and the corresponding cluster ions. By far, most of the molecular ions have been formed by one-step reactions; exceptions are eventually the $CO_4H_m^-$ ions created by a reaction between CO_3^- and water molecules. An intense mass line corresponding to HCO_3^+ has been observed, but not the one due to formaldehyde ion. Weak signals of ionic ketene, hydrogen peroxide and carbonic acid were seen.

Keywords: Secondary ions; Condensed gases; CO_2–H_2O ice; Electronic sputtering; TOF SIMS; PDMS; Cluster desorption

1. Introduction

The aim of this work is to explore the production of organic ions in the nuclear track plasma and their emission into vacuum—processes which supposedly occur on the icy surfaces of planetary objects like the Jovian moons bombarded continuously by energetic ions out of the magnetosphere of Jupiter [1]. The present article is Part II of the study on electronic sputtering from a mixture of frozen CO_2 and H_2O gases at a temperature of about 80 K. The measurement of mass spectra of the secondary ions ejected from the CO_2–H_2O ice surface by 1.7 MeV N ions and by ^{252}Cf fission fragments (FF) was described in Part I [2]. It is recalled that the CO_2–H_2O vapor mixture was condensed on an Al foil. For the case of positive ion ejection, the results were obtained by using 9 or 18% concentration of H_2O in the ice; while for the case of negative ions, this concentration was ∼5% [2]. The corresponding total yields ions are found to be 0.35, 0.57 and 0.066 ions/impact, respectively. The results displayed in Part I reveal complex mass spectra of positive as well as negative ions. They were separated into spectra of CO_2 specific ions, H_2O specific ions and the hybrid molecular ions. The H_2O specific ions, particularly the cluster series

---

* Corresponding author. Tel.: +55 213114 1272; fax: +55 213114 1040.
E-mail address: enio@vdg.fis.puc-rio.br (E.F. da Silveira).

[1] Guest of the Institute of Nuc1ear Physics, Technical University, 64289 Darrnstadt, Germany.

1387-3806/$ – see front matter © 2005 Elsevier B.V. All rights reserved.
doi:10.1016/j.ijms.2005.04.002

$(H_2O)_nH_3O^+$, were subject of recent investigations of ion emission from pure water ice [3].

In the following, mainly the hybrid molecular ions – the third group of ions – are addressed. The chemical designation of the observed ions is proposed and justified; then the ion formation processes and possible chemical reactions are discussed.

2. Chemical designation

The atomic composition of the observed molecular ions is evaluated under the assumption that their constituents are only C, O and H atoms. It turns out that the mass differences 18 u (H_2O mass) and 44 u (CO_2 mass) appear very often in the mass spectra; in fact, all ions above $m = 80$ u are members of cluster series starting at lower masses. The low mass regions of spectra measured for positive and negative ions by means of 1.7 MeV N ions are shown in Figs. 1a and 2a. Each mass line is assigned by its proposed chemical designation.

2.1. Positive ions

Hydrocarbon groups $C_nH_m{}^+$, typical for secondary ion mass spectra of organic material, are not observed. An exception is the group $(CH_{m=0\text{–}3})^+$ whose origin is discussed in the next section.

Above $m = 63$ u, all mass lines of positive ions represent ions of type:

$$(H_2O)_m(CO_2)_nR^+ \quad \text{with } R^+ = H^+, C^+, O^+, O_2{}^+, CO^+, CO_2{}^+ \qquad (1)$$

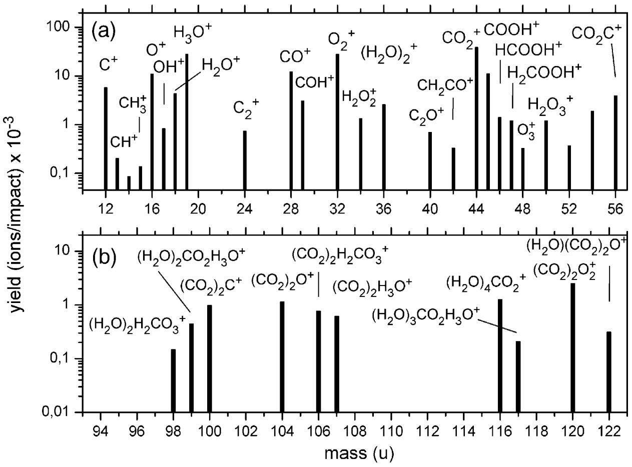

Fig. 1. Chemical designation in the mass spectrum of positive secondary ions ejected from CO_2–H_2O (9%) ice by 1.7 MeV N^{2+} ions. (a) Low mass region. The designation of the mass lines at $m = 52$ and 54 u is $(H_2O)H_2O_2{}^+$ and $(H_2O)_3{}^+$, respectively. Two strong mass lines at $m = 37$ and 55 u attributed to the H_2O specific ions ($(H_2O)H_3O^+$ and $(H_2O)_2H_3O^+$) were removed; (b) medium mass region. Again, two strong mass lines at $m = 109$ and 127 u of H_2O specific ions ($(H_2O)_5H_3O^+$ and $(H_2O)_6H_3O^+$) were removed.

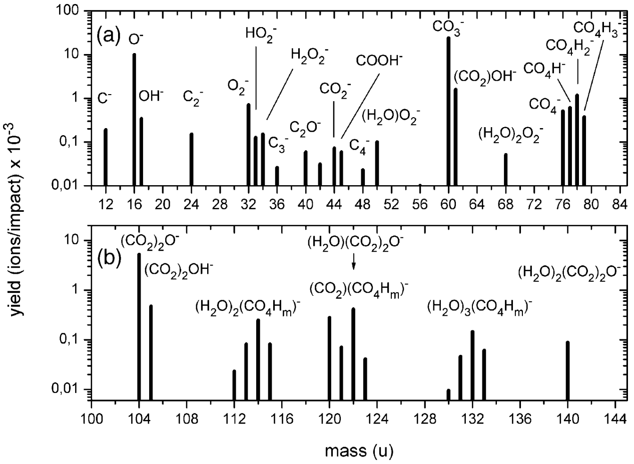

Fig. 2. Chemical designation in the mass spectrum of negative secondary ions ejected from CO_2–H_2O (∼5%) ice by 1.7 MeV N^{2+} ions. (a) Low mass region. The designation of the mass lines at $m = 42$ u is CH_2CO^-; (b) medium mass region. The mass lines at $m = 122$ u are composed of two ionic species, $(H_2O)(CO_2)_2O^-$ and $(CO_2)(CO_4H_2)^-$.

An example for the applicability of this expression is presented in Fig. 1b. Expression (1) includes CO_2 specific cluster ions with $m = 0$ and $R^+ = C^+, O^+, O_2{}^+, CO^+, CO_2{}^+$, which are listed in Part I of this work, Table 2 [2]. The subscripts m and n vary from 0 to 5 and from 0 to 4, respectively, but not all possible combinations (m, n) were observed. Here, it is assumed that molecules CO_2 and H_2O, being constituents of clusters $(H_2O)_m$ and $(CO_2)_n$, keep their identity. As it is discussed in the next section, the general expression (1) does not always display the actual chemical structure of a hybrid molecular ion. As examples, the species $HCOOH^+$ can also be written as $(H_2O)CO^+$, the ion $(CO_2)_2H^+$ is probably better characterized by $(CO_2)COOH^+$ as well as $(H_2O)_m(CO_2)_nH^+$ is by $(H_2O)_{m-1}(CO_2)_nH_3O^+$. The positive hybrid molecular ions are listed together with their yields in Table 1.

2.2. Negative ions

The common C_nH^- negative hydrocarbon ions are not observed in the CO_2–H_2O samples. The negative ions with high mass ($m > 79$ u) also exhibit a clustered structure, which can be characterized by the expression (yields are given in Table 2):

$$(H_2O)_m(CO_2)_nR^- \quad \text{with } R^- = O^-, OH^-, O_2{}^- \text{ and } (CO_4H_{m=0\text{–}3})^- \qquad (2)$$

The Fig. 2b shows a region of a mass spectrum of negative ions for which this designation is applied. The four-finger structure of the $(CO_4H_{m=0\text{–}3})^-$ group seen in Fig. 2a is frequently repeated in the mass range above $m = 80$ u. The values of m and n observed experimentally are presented in Table 2. Two weak mass lines at $m = 181$ and 282 u did not fall into the designation pattern of expression (2).

Table 1
Yields of positive (hybrid and specific) molecular ions

Projectiles	Yield ions/impact ($\times 10^{-3}$)				Masse (u) or *n*
	1.7 MeV N^{2+}	1.7 MeV N^{2+}	0.66 MeV	FF	
H_2O-concentration	9%	18%	≅10%	≤10%	
H^+					
OH^+	0.56	0.73	0.05	8	17
COH^+	3.1	9.1	0.6	160	29
$COOH^+$	11	10	0.5	180	45
$(CO_2)COOH^+$	3.1	1.0	0.3	50	89
$(CO_2)_2COOH^+$	0.81	2.0			133
H_3O^+					
H_2COOH^+	1.2	4.3			47
$CO_2H_3O^+$	2.1	3.4		65	63
$(CO_2)_nH_3O^+$	3.2	6.0			1–3, 5
$(H_2O)_m(CO_2)H_3O^+$	2.0	5.9	1.1 ($m = 1$–5)	100 ($m = 1$–5)	1–3
$H_2O(CO_2)_2H_3O^+$	0.50	0.58			125
C^+					
$C_2{}^+$	0.74	0.04	0.1	32	24
CH^+	0.20	0.05	<0.03	7	13
$CH_2{}^+$	0.08	<0.03	<0.05	≤3	14
$CH_3{}^+$	0.14	0.16	<0.1	5	15
O^+					
C_2O^+	0.69	2.2			40
$H_2O_2{}^+$	1.3	1.1			34
$(H_2O)H_2O_2{}^+$	0.37				52
$H_2O(CO_2)_2O^+$	0.31	0.52			122
$O_2{}^+$					
$O_3{}^+$	0.33	0.012			48
$H_2O_3{}^+$	1.9	4.0			1.2
$H_2O(CO_2)_2O_2{}^+$	0.22	0.68			138
CO^+					
$HCOOH^+$	1.4	1.9			46
$CO_2{}^+$					
$H_2CO_3{}^+$	0.99	1.9			62
$(H_2O)_2H_2CO_3{}^+$	0.15	0.43			98
$(H_2O)_m(CO_2)_nH_2CO_3{}^+$	2.0	2.6			$m = 0, 1, n = 1, 2$

Yields of cluster ions belonging to the same series have been summed over the given *n*. This table contains the hybrid ions (those formed from both ices), and the CO_2 and H_2O specific ones (i.e., those originated from just one ice species).

3. Discussion

A 1.7 MeV N ion penetrating in CO_2–H_2O (9%) ice deposits an energy of about 160 eV per monolayer into the electronic system of the solid, i.e., into ionization and electron excitation of atoms and molecules. A large number of positive ions are produced via direct projectile-ice coulomb interaction; further positive ions are produced by δ-electron impact and Auger processes. Electrons generated by these processes energize the surroundings of the nuclear track, and after thermalization, are trapped in the conduction band and at defect sites—in particular at atoms or molecules having a high electron affinity (O^-, OH^-). It could be estimated, with help of experimental data and expressions given in ref. [4], that the volume of sputtered ice accounts for an equivalent of 1600 CO_2–H_2O molecules per impact and that the number of ionic particles primarily produced inside this volume is 1–2 orders of magnitude lower than 1600. Within the time of the inverse electron plasma frequency ($<10^{-15}$ s), the positively charged particles are rapidly neutralized by electrons from the conduction band. It is assumed that only the primarily ionic particles have a chance to survive as charged species, which can escape into gas phase, i.e., directly into vacuum or into the highly excited and fast expanding cloud of particles at the track exit. The number of these ions is very small, as seen in Part I, Table 1 [2]: less than one ion is produced per impact, compared to about 2000 neutral particles per impact.

In the cloud of ejecta, the few relatively high energetic primarily produced ions can undergo suprathermal chemical reactions [5]. Energy distributions of small fragment ions ejected from organic solids bombarded by high energetic ions had mean energies in the order of 1 eV [6]. The present TOF spectra show that the width of mass lines observed for most negative ions is generally about 30% smaller than that of positive ions. This means that the negative ions seem to be colder than the positive ions, as they are generated by electron

Table 2
Yields of negative hybrid molecular ions

Projectiles	Yield (ions/impact × 10^{-3})		
	1.7 MeV N^{2+}	0.86 MeV N^{2+}	^{252}Cf FF
H_2O concentration	∼5%	≅10%	≅10%
OH^-	0.34	0.6	28
$(CO_2)_{n=1–6}OH^-$	2.4		48 (n = 1–13)
$COOH^-$	0.06		
CH_2CO^-	0.03		
$HO_2{}^-$	0.13		
$H_2O_2{}^-$	0.15		
$(H_2O)_{n=1–3,6}O_2{}^-$	0.27		
$(H_2O)_{n=1,4}(CO_2)_2O^-$	0.14		
$CO_4{}^-$	0.51	0.16	12.7
$(H_2O)_{n=1–6}CO_4{}^-$	0.22		
$(CO_2)_{n=1–5}CO_4{}^-$	0.53		
$HCO_4{}^-$	0.61	0.26	18.9
$(H_2O)_{n=1–6}HCO_4{}^-$	0.54		
$(CO_2)_{n=1–5}HCO_4{}^-$	0.20		
$H_2CO_4{}^-$	1.16	0.44	25.4
$(H_2O)_{n=1–6}H_2CO_4{}^-$	1.2		
$(CO_2)_{n=1–5}H_2CO_4{}^-$	1.03		
$H_3CO_4{}^-$	0.37	0.30	10.9
$(CO_2)_nO^-$	0.46		
$(CO_2)_{n=1–5}H_3CO_4{}^-$	0.24		

Yields of cluster ions belonging to the same series have been summed over the given n.

capture [7] whereas the positive ions have experienced the coulomb repulsion in the track core. The fact that the total yield of positive ions is one order of magnitude higher than that of the negative ones is probably related to their higher escape velocity, which reduces their neutralization probability.

3.1. Positive ions

Regarding the general pattern of the measured TOF spectra, one notices that most of the positive ion intensity is concentrated in atomic or small molecular ions $R^+ = H^+$, C^+, O^+, CO^+, $O_2{}^+$, $CO_2{}^+$ and in ionic reaction products of type $(H_2O)_m(CO_2)_n$ R^+ with $m = 0, 1, 2, \ldots$ and $n = 0, 1, 2, \ldots$ The R^+ ions react with the most abundant molecules in the nuclear track plasma—that is, H_2O and CO_2, either isolated or clustered. Also carbon monoxide CO, an often reported radiolysis product of CO_2, serves as a reaction partner leading to CO–R^+. Moreover, the general chemical expression (1) suggests that most of the observed ions are formed by one-step reactions. The time during which the reaction occurs has to be shorter than 10^{-10} s. Longer reaction times would lead to delayed emission indicated by tails of mass lines, which were not observed.

The formation of the R^+ ions and H_2O specific ions is discussed first, and then the formation of the CO_2 specific ions and of the hybrid molecular ions.

3.1.1. H^+, H_3O^+ and H_2O^+

The H^+ and H_3O^+ are specific ions for H_2O ice and have been analyzed in ref. [2]. H^+ is certainly a very abundant particle in the track core and gains kinetic energy by coulomb repulsion. It reacts preferentially with H_2O to form H_3O^+, the hydronium ion [8], in which all the three proton bonds are indistinguishable. In Table 1, H_3O^+ is treated as an R^+ ion reacting with neutral molecules. The resulting ion is then formed by a two-step reaction: (a) the proton is first captured by H_2O, forming H_3O^+ and then (b) the neutral molecule reacts with the H_3O^+. However, it cannot be excluded that H_3O^+ is formed in H_2O-containing complexes by proton capture. The advantage of the latter process would be that the final ionic reaction product is reached by only one-step reaction.

H_2O^+ is seldom seen in TOF spectra measured with MeV N ions bombarding pure water ice [3]. On the other hand, spectra taken with CO_2–H_2O ice exhibit a relatively strong H_2O^+ intensity: as seen in Fig. 3, the H_2O^+ yield increases with H_2O concentration, the increase being stronger than that of the H_3O^+ yield. Furthermore, in the case of 9% H_2O concentration, the H_2O^+ line is broadened in the direction of shorter flight times. Such a broadening indicates higher ejection energies, i.e., atomic collision sputtering. The tail of the H_2O^+ line is less expressed than that of the O^+ line (see discussion of O^+ below), because for high collision energies the H_2O^+ molecule dissociates. This means that the "axial" energy (E_a) distribution of the ejected H_2O^+ molecules decreases steeper than with E_a^{-2} (see, for instance [6]). The question that arises, however, is: why such a tail is not observed for an H_2O concentration of 18%?

The Fig. 6 of ref. [3] illustrates that the H_2O^+ yield increases sharply when the water ice layer has disappeared by sublimation and the remaining H_2O molecules are bound directly to the Al or Al_2O_3 surface of the target carrier. Therefore, it is reasonable to conclude that H_2O^+ is produced mainly via direct coulomb interaction of water molecules with the MeV N ions. This may occur primarily in water ice; as the formed H_2O^+ is linked to a neighboring H_2O by

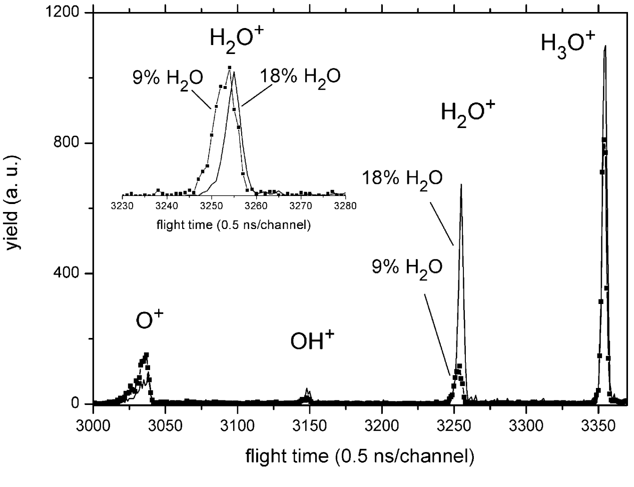

Fig. 3. Comparison of low mass parts of TOF spectra measured with 9 and 18% H_2O concentration and a 1.7 MeV N^{2+} beam. The corresponding ion yields are given in Table 1. The insert shows the H_2O^+ mass lines normalized to the same height.

hydrogen bond, the dissociation takes place:

$$(H_2O)H_2O^+ \rightarrow H_3O^+ + OH$$

In pure water ice, this transition leads to loss of H_2O^+ ions. The transition seems to occur only when there is a hydrogen bond to a neighboring water molecule.

Kosevich et al. [9] bombarded amorphous H_2O ice with 4–5 keV argon atoms at about 150 K. Their FAB mass spectrum is essentially composed only by H_3O^+, H_2O^+ and OH^+, indicating that the H_2O^+ ions are produced above the sample surface in a cloud of subliming water molecules by gas-phase ionization. This explanation certainly does not hold for H_2O^+ emission from an ice-free target nor for ice temperatures of about 90 K. They also observed the strong H_2O^+ intensity only at ice temperatures somewhere between 140 and 170 K. At about 130 K amorphous ice turns into a viscous liquid and the hydrogen bonds redistribute rapidly. We suggest that the binding of H_2O^+ to other water molecules is hindered in this temperature range and therefore so does the transition from H_2O^+ to H_3O^+.

3.1.2. C^+, CO^+, $O_2{}^+$, $CO_2{}^+$

These ions are probably formed by projectile-target direct interaction; the first three species are dissociation products of CO_2. All the four ion species seem to follow the same formation process, since the ratio of their yields measured with 9 and 18% H_2O concentration in the ice is the same, 1.5 ± 0.1 (Table 2 [2]) and their yield curves have the same slope (Fig. 9a of ref. [2]). However, the yield curve of $O_2{}^+$, above 80% CO_2 concentration, is less steep than that of the C^+, CO^+, $CO_2{}^+$ curves, indicating an influence of H_2O. For pure H_2O ice, the yield of $O_2{}^+$ was found to be very low [3].

3.1.3. O^+

Oxygen is very abundant in the ice mixture. As seen in Fig. 3, independently of the H_2O concentration, the O^+ mass line has a tail to shorter flight times being typical for atomic collision sputtering (see, for instance, ref. [6]). This is consistent with the finding that both H_2O ice and CO_2 ice contribute to the O^+ yield. For CO_2 concentrations above 50%, the O^+ yield is practically equal to the C^+ yield, while for lower concentrations the H_2O contribution for the O^+ yield becomes visible (Fig. 9a [2]). Such behavior supports the conclusion that O^+ stems mainly from CO_2 ice.

3.1.4. Positive hybrid molecular ions

The primarily produced ions R^+ react with the constituents of the nuclear track plasma and form H_2O specific reaction products, CO_2 specific reactions products [2] and hybrid ions (Tables 1 and 2). The yield of the positive hybrid molecular ions accounts for 12% of the total positive ion yield, in the case of 9% H_2O concentration in the ice, and for 8%, in the case of 18% H_2O concentration. The difference is mainly attributed to the difference of H_2O specific ion yields.

In Table 1, two groups of molecular ions are listed: first those which are produced by reactions between $R^+ = H^+$, H_3O^+ and CO_2 or CO, and second those between $R^+ = C^+$, O^+, CO^+, $O_2{}^+$, $CO_2{}^+$ and H_2O. We propose the following basic reactions:

$$H^+ + CO \rightarrow HCO^+$$

$$H^+ + CO_2 \rightarrow COOH^+$$

$$H_3O^+ + CO \rightarrow H_2COOH^+$$

$$H_3O^+ + CO_2 \rightarrow H_2CO_3H^+$$

$$O^+ + H_2O \rightarrow H_2O_2{}^+$$

$$O_2{}^+ + H_2O \rightarrow H_2O_3{}^+$$

$$CO^+ + H_2O \rightarrow HCOOH^+$$

$$CO_2{}^+ + H_2O \rightarrow H_2CO_3{}^+$$

These eight product ions have been detected—in the case of 9% H_2O concentration they account for 54% of the yield of the hybrid ions and, in the case of 18% H_2O, for 70%. The reacting CO_2 and H_2O can be members of clusters $(H_2O)_m(CO_2)_n$. Then, the eight product ions can be incorporated into the clusters. Generally, the longest cluster series are those which are composed of only water or only carbon dioxide molecules. The hybrid cluster series observed contain no more than four constituents, probably because the binding energy between CO_2 and H_2O is smaller.

As seen in Table 1, on the average the yields of most hybrid ions increase with H_2O concentration. In Fig. 4a, yield curves of COH^+, $COOH^+$, $(CO_2)COOH^+$ and $(CO_2)H_3O^+$

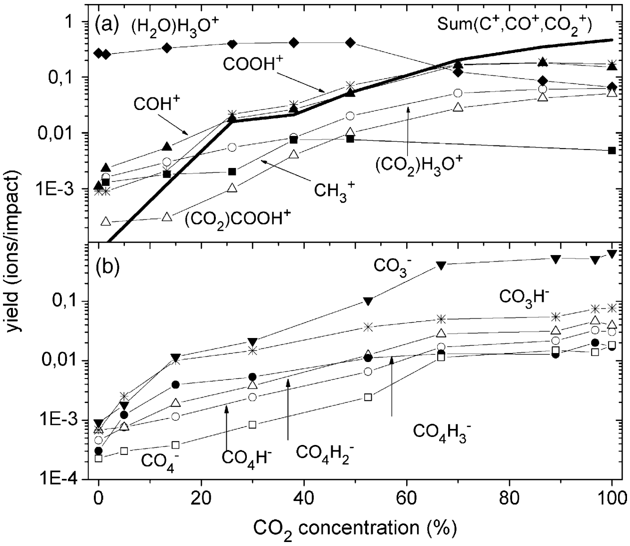

Fig. 4. Yields of hybrid molecular ions measured as function of CO_2 concentration and compared with those of CO_2 and H_2O specific ions. The ice targets were irradiated by fission fragments. (a) Yield curves of positive ions. The thick curve was deduced from the sum of yields obtained for C^+, CO^+ and CO_2+; (b) yield curves of negative ions.

are compared with an average curve of CO_2 specific primarily ions. As expected, the slope of the curves decreases as the CO_2 concentration increases, i.e., the H_2O concentration declines. Towards low CO_2 concentrations, the slope of the $(CO_2)H_3O^+$ curve decreases less than that of the other curves, indicating a high reaction probability of the dominant H_3O^+ with the decreasing number of CO_2 molecules. An exceptional behavior occurs for the $O_3{}^+$ ion: its yield decreases with H_2O concentration (from 9 to 18%) because the two reaction partners O and $O_2{}^+$ or O^+ and O_2 both originate from CO_2. An opposite example is the ion at mass 36 u (Fig. 1): its yield increases by a factor of 4.5 with H_2O concentration indicating that $m = 36$ u is attributed mainly to $(H_2O)_2{}^+$, but not to $C_3{}^+$. Note that yield curves such as those shown in Fig. 4 can be indeed used to reveal certain reaction pathways.

The only ions with distinct C–H bonds are CH^+, $CH_2{}^+$ and $CH_3{}^+$. Their yields are low, but clearly above background. In mass spectra measured within the electronic sputter regime, these ions appear as fragment ions of organic compounds, but usually with very low yields ([10]; see also Fig. 2 of ref. [2]). The yield of $CH_3{}^+$ increases steadily up to 50% CO_2 concentration, as seen in Fig. 4a. It is supposed that the CH^+, $CH_2{}^+$ and $CH_3{}^+$ ions are generated via a reaction scheme C/H_2O, as discussed by Roessler [5]. This scheme would lead to methane, which can hardly be resolved as $CH_4{}^+$ ion from O^+ ($\Delta m = 0.044$ u). On the other hand, the TOF spectrum of frozen methane irradiated by ^{252}Cf fission fragments shows a very weak $CH_4{}^+$ ion peak, while the $CH_3{}^+$ ion at $m = 15$ u is intense [11]. The scheme of Roessler et al. predicts in addition H_2CO ($m = 30$ u), H_2COH ($m = 31$ u) and CH_3OH ($m = 32$ u). The formation of the two heavier molecules require more than one step, as their yields might be too small for detection. The ion with mass 30 u was not observed, so its yield has to be below 0.07×10^{-3} ions/impact, the yield detection limit for this mass region. However, the H_2CO (formaldehyde) has been deduced from absorption bands investigated by infrared spectroscopy [12,13] and also by quadrupole mass spectrometry as a neutral molecule sublimating from CO_2–H_2O ice, when irradiated by 1.5 MeV helium ions [14]. The $m = 29$ u would correspond to the de-protonated formaldehyde ion, COH^+, which has one of the more intensive yields in Table 1. A mass line of the methanol ion $(CH_3OH)^+$ would be superposed by the strong $O_2{}^+$ line.

The molecular ions COH^+, $COOH^+$ and C_2O^+ have not been reported so far, probably because they react with the surrounding ice matrix soon after formation. Absorption bands corresponding to CO–R and C_2O were reported by Moore et al. [15], and CO–R with low confidence by Benit et al. [13]. Other interesting ions are H_2COOH^+ and $HCOOH^+$. They have not been observed by other methods so far. A molecular ion seen in the spectrum of Fig. 1a is $H_2CO_3{}^+$, the positive ion of carbonic acid. It appears also protonated or as a hydrated complex $(H_2O)_2H_2CO_3{}^+$. By means of infrared spectroscopy the formation of H_2CO_3 in CO_2–H_2O ice by proton irradiation was confirmed by DelloRusso et al. [12]. The molecular ion of ketene, CH_2CO^+ at $m = 42$ u, has also a low yield, relatively close to the detection limit. Thus, the chance to produce acetic acid, CH_3COOH, via a reaction with H_2O is low. A corresponding mass line at $m = 60$ u was found, but it belongs to $(CO_2)O^+$, a CO_2 specific ion [2].

The ion $H_2O_2{}^+$ observed with relatively low yield is considered a hybrid molecular ion because it is formed with help of O^+, a primarily ion originating mainly from CO_2. Its yield does not increase with H_2O concentration in the ice. Hydrogen peroxide was detected by means of mass spectroscopy as a sputter product from pure water ice being irradiated by heavy 3 keV ions [16]. It reacts with OH to form the radical HO_2 which, however, has not been seen as an ion in the present mass spectra. ($Y_{\mathrm{lim}} = 0.07 \times 10^{-3}$ ions/impact).

3.2. Negative ions

The yield of negative ions produced by MeV ion impact is smaller than the yield of positive ions. For pure H_2O ice, the positive and negative ion total yield ratio is about 25 [3]. For CO_2 ice (<10% H_2O concentration), this ratio is about 5 [2]. Therefore, the production of negative ions by MeV ion impact seems to be generally much higher in CO_2 ice than in H_2O ice. The reason for this is probably the capture of free electrons generated along the nuclear track by oxygen atoms and the chance of O^- and negative reaction products of O^- to survive neutralization, i.e., to escape into gas phase as charged species. The negative ion spectrum is then dominated by the O^- ion and its reaction products.

3.2.1. O^-, $O_2{}^-$

Compared with the mass line of O^+, the mass line of O^- exhibits only a small tail to shorter flight times—this means that most negative oxygen ions are thermalized before emission (the fraction generated by atomic collisions is about 10%). The yields of O^- and O^+ are almost equal, but the kinetic energy of O^+ is distinctly higher than that of O^-; accordingly, O^+ is less involved in reactions than O^-.

The yield curves of the O^- ion, as well as that of the low intense $O_2{}^-$ ion peak, follow the same slope as that of $C_2{}^-$, a pure CO_2 derivate (Fig. 9b of ref. [2]). Therefore, at 9 and 18% H_2O concentrations, both ionic species should originate mainly from CO_2 ice. For pure water ice, the yields of O^- and $O_2{}^-$ measured with fission fragments [3] are 30 and 200 times, respectively, lower than those obtained for pure CO_2.

3.2.2. OH^-

This ion is listed in ref. [2], Table 3, as an H_2O specific ion, but regarding its yield curve (not shown), the OH^- yield measured with fission fragment irradiation increases steadily up to 50% CO_2 concentration and drops then similarly to the curves of H^- and $(H_2O)O^-$. The O^- ions appear to react with water molecules as

$$H_2O + O^- \rightarrow OH + OH^-$$

3.2.3. CO_3^-, $(CO_2)_nO^-$

The negative ion spectra measured for CO_2–H_2O ice by MeV N ions and fission fragments are dominated by the CO_3^- ion and the cluster series $(CO_2)_nO^-$ (Fig. 6 and Table 2, ref. [2]). The $(CO_2)_nO^-$ series can also be designated as $(CO_2)_{n-1}CO_3^-$ and can be reached by a one step reaction of a $(CO_2)_n$ cluster with O^-. As seen in Fig. 9 of ref. [2] and in Fig. 4b, the very pronounced dependence of the CO_3^- yield on the CO_2 concentration indicates that two CO_2 specific atoms or molecules are involved in the reaction forming CO_3^-. We suggest the reaction

$$CO_2 + O^- \rightarrow CO_3^-$$

The molecule CO_3 has been observed by Gerakines et al. [17] and Benit et al. [13] using H^+ and He^+ beams for irradiation of CO_2–H_2O ice and infrared spectroscopy. The spectra displayed in Fig. 5b of ref. [2] show a weak CO_3^+ signal, whereas the CO_3^- signal is 22 times stronger. Its reaction with water would lead to carbonic acid, H_2CO_3, which has been reported by several authors [10]. In Fig. 2 of ref. [2], it is seen a stronger signal at $m = 61$ u, which can be designated as CO_3H^+, and a weak positive ion signal at $m = 62$ u, the mass of H_2CO_3. The double charged anion CO_3^{2-} of the carbonic acid at $m/2 = 30$ u has not been observed.

3.2.4. Negative hybrid molecular ions:

The observed hybrid ions are listed in Table 2. Similarly to O^-, OH^- reacts with $(CO_2)_n$ clusters to form the series $(CO_2)_nOH^-$, whose intensity is about seven times smaller than that of the $(CO_2)_nO^-$ series. The basic reaction is:

$$CO_2 + OH^- \rightarrow (CO_2)OH^-$$

In the low mass range ($m \leq 50$ u), several low intensity ions – $(C_{n=1\text{–}4})^-$, $H_2O_2^-$, C_2O^-, CH_2CO^-, CO_2^-, $COOH^-$ and $(H_2O)O_2^-$ – are observed, which are also found as positively charged molecules in the positive mass spectrum presented in Fig. 1a. In a few cases, OH^- and O^- are adducted to $(H_2O)_m(CO_2)_n$ clusters.

The cluster series C_n^- is even less expressed than the C_n^+ series. Compared with O or to O attached to a R group, the electron affinity of $C_n > 2$ clusters is high, 2–5 eV [19]. This means that the density of such clusters around the nuclear track should be low—much lower than that of O and OR, which consume the available free electrons. The formation of carbon clusters in the nuclear track plasma is a well known phenomenon—TOF spectra of negative ions ejected from pure frozen hydrocarbon compounds consist mainly of the four-finger groups $(C_nH_{m=0\text{–}3})^-$ [10]. The strongest signals are those of C_nH^- for even n. Corresponding groups of ions were not observed in the present spectra. The $(C_nH_{m=0\text{–}3})^-$ ions were also reported for targets of frozen acetone irradiated by fission fragments [20].

3.2.5. $(CO_4H_m)^-$ with $m = 0$–3 and corresponding clusters

The most interesting negative molecular ions ejected from CO_2–H_2O ice by MeV N ions as well as by fission fragments are the ions of the group $(CO_4H_m)^-$ with $m = 0$–3. The spectral pattern of this group and the corresponding cluster ions are seen in Fig. 2a and in Fig. 8 of ref. [2]. Ion yields are listed in Table 2.

As mentioned, four-finger groups of negative ions are typical for mass spectra of frozen organic samples. They are explained by the number of C–H bonds of carbon cluster ions $C_nH_m^-$ being formed in the nuclear track plasma. Clusters C_n^- have four free carbon bonds, when, for instance, the carbon chain is linear and the adjacent carbon atoms are connected by double bonds. Since one bond is occupied by the negative charge (an electron), $C_nH_m^-$ cluster ions are possible with $m = 0, 1, 2, 3$. For odd values of n, an acetylenic structure of C_n^- provides four free carbon bonds also. The four-finger group $m = 76$–79 u is 4 mass units too high to be assigned as $C_6H^-{}_{m=0\text{–}3}$. A cyclic $(OC_5H_{m=0\text{–}3})^-$ molecule, which would provide four C–H bonds, is not known. We suggest two possible reaction pathways leading to the four molecular ions $(CO_4H_m)^-$:

1. These ions are produced via reactions between CO_3^- and H_2O, the most abundant hydrogen containing molecule in the nuclear track plasma. In the hot track plasma CO_3 undergoes reactions with water molecules:

$$CO_3^- + H_2O \rightarrow CO_4^- + H_2 \quad (3)$$

$$CO_3^- + H_2O \rightarrow CO_4H^- + H \quad (4)$$

$$CO_3^- + H_2O \rightarrow CO_4H_2^- \quad (5)$$

$$CO_3^- + (H_2O)_2 \rightarrow CO_4H_3^- + OH \quad (6)$$

   The reactions (3)–(5) consume one H_2O molecule, reaction (6) two H_2O molecules. As seen in Fig. 4b, up to 53% CO_2 concentration, the reaction products $(CO_4H_{m=1,2,3})^-$ increase similarly to CO_3^-, then slower, due to the decreasing concentration of H_2O needed for reactions (3)–(5). The three yield curves $(CO_4H_{m=1,2,3})^-$ are almost parallel, and the reactions (3)–(5) seem to follow the same reaction pattern. To produce $CO_4H_3^-$ in reaction (6) a second water molecule is required. Therefore, due to the decreasing availability of two water molecules, the yield of $CO_4H_3^-$ bends down when the H_2O concentration becomes smaller.
2. Note that the $CO_4H_3^-$ yield behaves similarly to the yield curve of $(CO_2)OH^-$. The slope of the later reflects the availability of OH^-. A reaction leading to CO_4H_3 and consuming OH^- would be $H_2CO_3 + OH^-$. Carbonic acid is a transient compound formed in the heated CO_2–H_2O ice around the nuclear track. It reacts with the ions O^- and OH^- in the following way:

$$H_2CO_3 + O^- \rightarrow CO_4^- + H_2 \quad (7)$$

$$H_2CO_3 + O^- \rightarrow CO_4H^- + H \tag{8}$$

$$H_2CO_3 + O^- \rightarrow CO_4{H_2}^- \tag{9}$$

$$H_2CO_3 + OH^- \rightarrow CO_4{H_3}^- \tag{10}$$

The four yield curves of the $(CO_4H_m)^-$ (Fig. 4b) show in fact a dependence on the CO_2 concentration, which is similar to those of O^- and OH^-. Compared with reactions (3)–(6), the advantage of the reactions (7)–(10) is that the rare ionic reaction partners are involved in only one reaction step.

Above $m = 79$ u only series of negative cluster ions are observed, whose band heads are molecular ions with masses smaller than 80 u. These cluster series are listed in Table 2 of ref. [2] and in Table 2. Also the series of the $(CO_4H_m)^-$ group are well expressed as demonstrated in Fig. 2b.

A further discussion of the various possible reaction pathways is out of the scope of the present studies. They require in particular measurements capable to determine the precise relative composition of the ice, i.e., the ratio of the CO_2–H_2O abundance.

An attempt to summarize the positive and negative ion cluster structures is:

Molecular group		Ion group
$(H_2O)_m(CO_2)_n$	$m > 0$, $n > 1$	H_3O^+
$(H_2O)_m(CO_2)_n$	m and $n = 0$–2	${H_2CO_3}^+$
$(H_2O)(CO_2)_2O_k$	$k = 0, 1$	O^+
H_k or $(CO_2)_n$	k or $n = 0$–2	$COOH^+$
$(CO_2)_n$	$n = 0$–6	OH^-
$(H_2O)_m(CO_2)_n$	$m = 0$–4 and $n = 0$–2	O^-
$(H_2O)_m$	$m = 0$–$3, 6$	${O_2}^-$
$(H_2O)_m$	$m = 0$–6	$H_k{CO_4}^-$, $k = 0$–3
$(CO_2)_n$	$n = 0$–5	$H_k{CO_4}^-$, $k = 0$–3

The observed ion clusters are displayed in the form [molecular group][ion group]$^{+-}$. Remind that H_3O^+ was preferred to H_2O H^+ and that $COOH^+$ can also be CO_2 H^+.

4. Conclusions

The present TOF spectrometry detects those ions which are produced within 10^{-10} s after the heavy ion impact and which are ejected into vacuum. In contrast, infrared spectroscopy or quadrupole mass spectrometry is employed usually hours after irradiation to molecules which have been produced inside the target and which have experienced further chemical reactions. Thus, by the current method, it is seen mainly dissociation products of the ice constituents and products of reactions between these dissociation products and the most available molecules, CO_2 and H_2O, or clusters of them. Reactions between dissociation products themselves are rare; resulting molecules are, for instance, ${C_2}^+$, ${C_2}^-$, COH^+, $COOH^-$, CH_2CO^-, H_2COOH^+. One of the reaction partners is then H^+, C, O_2 or CO, all species, which are probably produced in large quantities along the nuclear track.

By far, most of the observed molecular ions are formed in one-step reactions. That is particularly true for positive ions, which have generally higher kinetic energies than the negative molecular ions. The primarily produced ions R^+ experience the Coulomb repulsion of the nuclear track, while the corresponding negative R^- have been generated by electron capture of thermalized atoms or molecules. The track plasma expands in very short time into vacuum [10] since its temperature is very high (between 3×10^3 and 10×10^3 K, according to values derived from energy distributions [6,21]). Therefore, the chance for multi-step reactions is low. For instance, the two most intensive radical ions COH^+ and $COOH^+$ resulted from one-step reactions. An exception is eventually the formation of $(CO_4H_m)^-$ which can be explained by two- or even three-step reactions.

Hydrocarbon ions ${C_nH_m}^+$ and ${C_nH_m}^-$ typical for TOF spectra of organic material [10] are hardly ever seen in the well resolved spectra. The ${C_nH_m}^+$ are usually fragments of organic ions. The ${C_nH_m}^-$ are supposed to be synthesized in the nuclear track plasma of atomized organic material, i.e., atoms and ions of hydrogen and carbon [10]. Such processes, however, seem to seldom occur in the track plasma of CO_2–H_2O ice. In particular, the yields of ${C_n}^+$ clusters are remarkably small. A recent investigation of pure CO ice (at 30 K) has shown that in this case clustered carbon atoms dominate the secondary ion spectrum [22].

Already our investigations of pure H_2O ice have shown that the patterns of the TOF spectra measured with MeV N ions and fission fragments are quite similar; differences can be explained by the more fragmentary processes in accordance with the higher temperature in the core of fission fragment tracks. This means that, concerning the production of new molecular ions, electronic sputtering is unique; the total yield of these ions depends linearly on the electronic energy loss, including a threshold of about 31 eV/Å [2].

The present experiment on CO_2–H_2O ice have shown that electronic sputtering accounts for the ejection of organic molecules from the icy surface. Of particular interest are the ions COH^+, $COOH^+$, ${CH_3}^+$ and ${CO_3}^-$, the first three being organic ions. For ice with 91% CO_2 concentration, they have yields of 0.0031, 0.011, 0.00014 and 0.019 ions/impact. Tables 1 and 2 exhibit various other organic ions, most having yields which are one order of magnitude lower than the ones above. At a CO_2 concentration of 1%, a more realistic for the icy surface layers of the Jovian moons, all the yields are supposedly two orders of magnitude smaller.

In the article of Delitsky and Lane [18] a list of further products of irradiation of CO_2–H_2O ice is published, such as H_2CO ($m = 30$ u), CH_2CO ($m = 42$ u), HCO ($m = 29$ u) and C_2O_3 ($m = 72$ u). Among these, the only ion which has been clearly identified in the present TOF spectra is HCO^+, the protonated CO molecule. The indications for organic compounds as ketene (CH_2CO) or formaldehyde (H_2CO), both observed by Benit et al. [13], are poor; they might appear in the TOF spectra as protonated or de-protonated molecular ions. Heavier, more complex organic ions cannot be expected, because the nuclear track plasma is too hot and fast expanding at the track exit.

Identification of new molecules, i.e., the hybrid molecular ions, was relatively straightforward. More problematic were ion yields measured for definite and small CO_2 concentration in the CO_2–H_2O ice. Disturbing was the modification of the ice surface by simultaneous condensation of the residual gas and introduced vapor mixture. The yields of hybrid molecular ions reach their maxima when the CO_2 content is between 50 and 80%. Therefore, measurements in the regime of low CO_2 concentrations (<20%) are needed. The method of TOF mass spectrometry developed for this work is capable of performing the task, provided that the rest gas pressure in the spectrometer chamber and in the mixing chamber is $\leq 10^{-9}$ mbar.

5. Comments

The present work (Parts I and II) aims to apply TOF SIMS to an astrophysical problem: the sputtering of planetary surfaces. Compared to other methods, TOF SIMS is a very sensitive method (nevertheless restricted to the charged component of the sputtered material): it detects the ions formed within 10^{-10} s after the projectile's impact. It is difficult to draw conclusions about the formation yield of a certain molecule by means of the corresponding desorption ion yield. The neutral molecule yield can be two to four orders of magnitude higher than the ion yield. A rough estimate leads then to 5–500 hybrid molecules per impact in the flux of sputtered particles for 1.7 MeV N projectiles and a CO_2/H_2O ratio of 1/1. In spite of the fact that the secondary ions represent a very small fraction of the sputtered flux, they probably reveal the whole spectrum of compounds, which are either ejected from the icy surface or formed in the ice bulk, the latter being produced inside the nuclear track plasma within 10^{-10} s after the projectile's impact. These new compounds react further with the CO_2–H_2O matrix or among themselves. The method employed here, TOF SIMS, can be also used to detect and identify the prompt (stable) products as well as such late products. It should be possible to detect them, when 1% of the irradiated material (the uppermost 50 nm) is converted into hybrid molecules. This requires a flux of $3 \times l0^{(12 \pm 1)}$ ions/cm^2 for a 1.7 MeV N^{2+} beam.

References

[1] R.E. Johnson, Energetic Charged Particles Interactions with Atmospheres and Surfaces, Springer-Verlag, Heidelberg, 1990.
[2] L.S. Farenzena, V.M. Collado, C.R. Ponciano, E.F. da Silveira, K. Wien, Int. J. Mass Spectrom. 243 (2005) 85.
[3] V.M. Collado, L.S. Farenzena, C.R. Ponciano, E.F. da Silveira, K. Wien, Surf. Sci. 569 (2004) 149.
[4] R.E. Johnson, in: R.A. Dressler (Ed.), Advanced Series in Physical Chemistry, 11, 2000, p. 390.
[5] K. Roessler, in: E. Bussorelli, G. Strazulla (Eds.), Suprathermal Chemistry in Space, in Solid State Astrophysics, North Holland, Amsterdam, 1991.
[6] G. Betz, K. Wien, Int. J. Mass Spectrom. Ion Processes 140 (1994) 1.
[7] E.F. da Silveira, M.G. Blain, E.A. Schweikert, J. Phys. 2 (1989) C2.
[8] P.A. Giguere, J. Chem. Educ. 56 (1979) 571;
see also R.L. Johnston, in: D.S. Betts (Ed.), Masters series in Physics and Astronomy, 2002, p. 64.
[9] M.V. Kosevich, O.A. Boryak, V.S. Shelkosky, V.V. Orlovv, Low Temp. Phys. 20 (2003) 805.
[10] M. Wagner, K. Wien, B. Curdes, E.R. Hilf, Nucl. Instrum. Methods B 82 (1993) 362.
[11] K. Wien, V. Obnorskii, in: H. Benninghoven (Ed.), Proceedings of the International Conference on Secondary Ion Mass Spectrometry, SIMS IX, Muenster, 1994, p. 199.
[12] N. DelloRusso, R.K. Khanna, M.H. Moore, J. Geophys. Res. 98 (1993) 5505.
[13] J. Benit, J.-P. Bibring, F. Rocard, Nucl. Instrum. Methods B 32 (1988) 349.
[14] V. Pirronello, W.L. Brown, L.J. Lanzerotti, K.J. Marcantonio, E.H. Simmons, Astrophys. J. 262 (1982) 636.
[15] M.H. Moore, R. Khanna, B. Donn, J. Geophys. Res. 96 (1991) 17541.
[16] A.E. de Vries, R.A. Haring, A. Haring, F.S. Klein, A.C. Kummel, F.W. Saris, J. Phys. Chem. 88 (1984) 4510.
[17] P.A. Gerakines, M.H. Moore, R.L. Hudson, Astron. Astrophys. 357 (2) (2000) 793.
[18] M.L. Delitsky, A.L. Lane, J. Geophys. Res. 10 (No. E7) (1997) 385.
[19] W. Weltner, R.J. Zee, Chem. Rev. 89 (1989) 1713.
[20] M. Wagner. Diploma Thesis, Inst. of Nucl. Physics of the Techn. Univers. Darmstadt, FRG, 1993.
[21] R.L. Betts, E.F. da Silveira, E.A. Schweikert, Int. J. Mass Spectrom. 145 (1995) 9.
[22] A. Naves de Brito, E.F. da Silveira, K. Wien, L.S. Farenzena. LNLS, Campinas, Internal Report, 2004.